Scientia Iranica A (2022) 29(3), 951–963

Sharif University of Technology
Scientia Iranica
Transactions A: Civil Engineering
http://scientiairanica.sharif.edu

Behavior of concentrically braced steel frames under fire loading

M.R. Kaffash[a], A. Karamodin[a,*], and M. Moghiman[b]

a. *Department of Civil Engineering, Ferdowsi University of Mashhad, Mashhad, Iran.*
b. *Department of Mechanical Engineering, Ferdowsi University of Mashhad, Mashhad, Iran.*

Received 1 February 2020; received in revised form 14 April 2021; accepted 25 October 2021

KEYWORDS
Concentrically braced frames;
Fire resistance;
Multi-stage analysis;
Macro-model;
Overall behavior.

Abstract. The necessity to better understand how a steel structure behaves under fire loading has gained significance, since a large number of recent events have proved the vulnerability of steel structures under such hazard. Older concentrically braced frames have been widely used in buildings, which had been formerly designed without observing seismic provisions and details. Although the vulnerability of this type of structural systems, here referred to as non-seismic braced frames, under earthquake loading has already been studied, its behavior under fire loading has not been investigated yet. Therefore, this study aims to investigate the behavior of global and local responses of the mentioned structural system under various uniform fire scenarios. The heating and cooling phases of fire were taken into account for different building stories using the finite element method. The results of the conducted analyses demonstrated that the braces buckled at high temperatures due to large compressive axial forces and expansion of lateral constraints. This phenomenon led to early loss of the lateral resistance of stories, which, in turn, resulted in the failure of columns. Consequently, the underlying floor collapsed under fire. The analysis results contributed to a better understanding of the behavior of steel braced frames under fire conditions.

1. Introduction

Many historical fire catastrophes have occurred for steel structures, resulting in their damage and, even, collapse as well as other subsequent fatalities. In addition, current codes and design guidelines lack enough information on the response of steel structures to fire loading in real events. Therefore, the response of steel structures to fire loading has drawn considerable attention in recent years. There are a large number of numerical and experimental studies on the behavior of steel moment-resisting frames, their connections, and individual structural steel elements under fire conditions [1–6]. Furthermore, numerical techniques are employed to investigate the progressive collapse and global stability of steel frame structures subjected to fire loading [7–11]. Moreover, several plastic and elastoplastic methods have been proposed to determine the critical temperature distribution over structures during fire exposure [12,13].

Some researchers have conducted several case studies on the effect of fire on steel structures. Fang et al. [14–16] studied modeling of a multi-story parking structure under fire from a vehicle. Lange et al. [17] proposed two collapse mechanisms for multi-story steel buildings when subjected to fire on different floors. Sun et al. [8,18] carried out analyses of a progressive collapse of steel moment frames with a combined hat and vertical bracing system under fire conditions. Behnam [19] conducted a series of sensitivity analyses on tall moment-resisting frames with the main focus

*. *Corresponding author. Tel.: +98 51 38805046*
E-mail address: a-karam@um.ac.ir (A. Karamodin)

doi: 10.24200/sci.2021.55367.4191

on the possibility of structural failure. In another research, a 16-story steel building in Tehran, Plasco Building, was investigated by Behnam [20] to understand the failure mechanism of the building. Memari and Mahmoud [21] investigated the steel frames with RBS connections using a multi-resolution modeling technique. Lou et al. [22] carried out experimental investigations into the collapse behavior of a full-scale steel portal frame exposed to natural fires.

The response of concentrically braced frames under fire loading has not been studied yet. The latest existing practice for this system is Special Concentrically Braced Frames (SCBFs), where there is a need for high ductility under seismic loading. Before the year 1988, the seismic design of concentrically braced frames was drawn without requiring special structural detailing [23]. Preceding Non-seismic Concentrically Braced Frame (NCBF) design requirements do not establish a clear hierarchy of yielding and failure, thus resulting in an uncertain seismic response and high susceptibility to a connection failure, frame member damage, and soft story collapse relative to SCBFs. These structural systems (here referred to as NCBFs) are characterized by unreliable seismic performance. Their behavior under fire conditions and their potential for collapse have not been studied yet. In this regard, the present study performs a number of numerical simulations under different fire scenarios with different fire phases to evaluate the performance of a multi-story NCBF subjected to uniform fire. To make a comparison, the same structure was designed using an SCBF system, which was examined under the same loading and fire scenarios. The results of this study are conducive to a better understanding of the behavior of braced frames and their corresponding local and global responses.

2. Methodology

In order to simulate the fire scenarios, it is required to conduct multi-stage and sequential analyses. In the present study, the analysis was performed and elaborated in the following steps [24] using the finite element method in ABAQUS software [25]. In the first step, the static linear analysis was carried out where the structure was subjected to gravity loads. In the second step, the nonlinear implicit dynamic analysis was performed where the effects of temperature rise on the structural members subjected to fire were evaluated. ASCE 7–10 [26] gave simultaneous combinations of gravity loads and fire loading, as presented in Eq. (1):

$$W = 1.25DL + 0.5LL. \tag{1}$$

2.1. Material properties

In order to model the material behaviour of steel, an elastic, perfectly plastic material model was used. Variations of steel properties with temperature changes were modeled in line with EN 1993-1-2 [27]. Figure 1(a) shows the modulus of elasticity and strength changes for the models. In this figure, the modulus of elasticity decreases linearly with temperature ranging from 100°C to 500°C, after which the rate of decrement increases. In addition, the yield stress does not undergo changes until 400°C; however, at higher temperatures, it decreases rapidly. Figure 1(b)–(d) present the thermal expansion, specific heat, and thermal conductivity changes, respectively. As seen in Figure 1(b), the coefficient of expansion of steel increases slowly until about 700°C and then, it decreases. Also, the relevant steel engineering properties were used for modeling the stress-strain behavior of steel in the analyses [28].

2.2. Fire load

Different temperature-time diagrams such as ISO 834-1 fire [29] and Eurocode fire diagram [27] are available that can be used for numerical simulation of fire loading. In this study, the diagram of Eurocode parametric fire, given by Eq. (2), was employed to implement the cooling phase and yield the temperature-time diagram as a function of fire load density, openings, and thermal characteristics of borders of fire compartment [30].

$$\theta = 20 + 1325\left(1 - 0.324e^{-0.2t^*} - 0.204^{-1.7t^*} - 0.472^{-19t^*}\right). \tag{2}$$

In this diagram, the temperature θ (°C) is a function of fictitious time t^*, obtained from the product $\Gamma \cdot t$ and Γ is a dimensionless parameter calculated by $(O/b)^2/(0.04/1160)^2$. In this relation, O denotes an opening factor and b the thermal absorptivity of compartment surfaces [30].

In this study, Γ is considered equal to unity to obtain a heating phase, which is close to that given by the ISO 834-1 standard fire diagram [31]. The heating phase which is approximated by ISO 834-1 fire diagram could be used for individual members as well as the frames. In this formulation, different design parameters such as fire load density ($q_{t,d}$), O, and b can be included in fire loading. The above parameters can be applied to both open-plan and closed-plan office buildings. For example, for an open-plan office building, $q_{t,d}$, O, and b parameters are equal to 130 MJ/m^2, 0.071 m$^{0.5}$, and 2030 J/(m^{2}s$^{0.5}$K), respectively; in the case of a closed-plan office building, the values of these parameters are 50 MJ/m^2, 0.027 m$^{0.5}$, and 783 J/(m^{2}s$^{0.5}$K), respectively [31]. According to Figure 2, Eq. (3) yields a maximum temperature equal to 800°C in 22 min for a combination of fire parameters for both open-plan and closed-plan office buildings:

$$t^*_{\max} = t_{\max} = \max\left\{0.2 \times 10^{-3}\frac{q_{t,d}}{O}, t_{\lim}\right\}. \tag{3}$$

If we take $t_{\lim}$ equal to 20 min for the medium

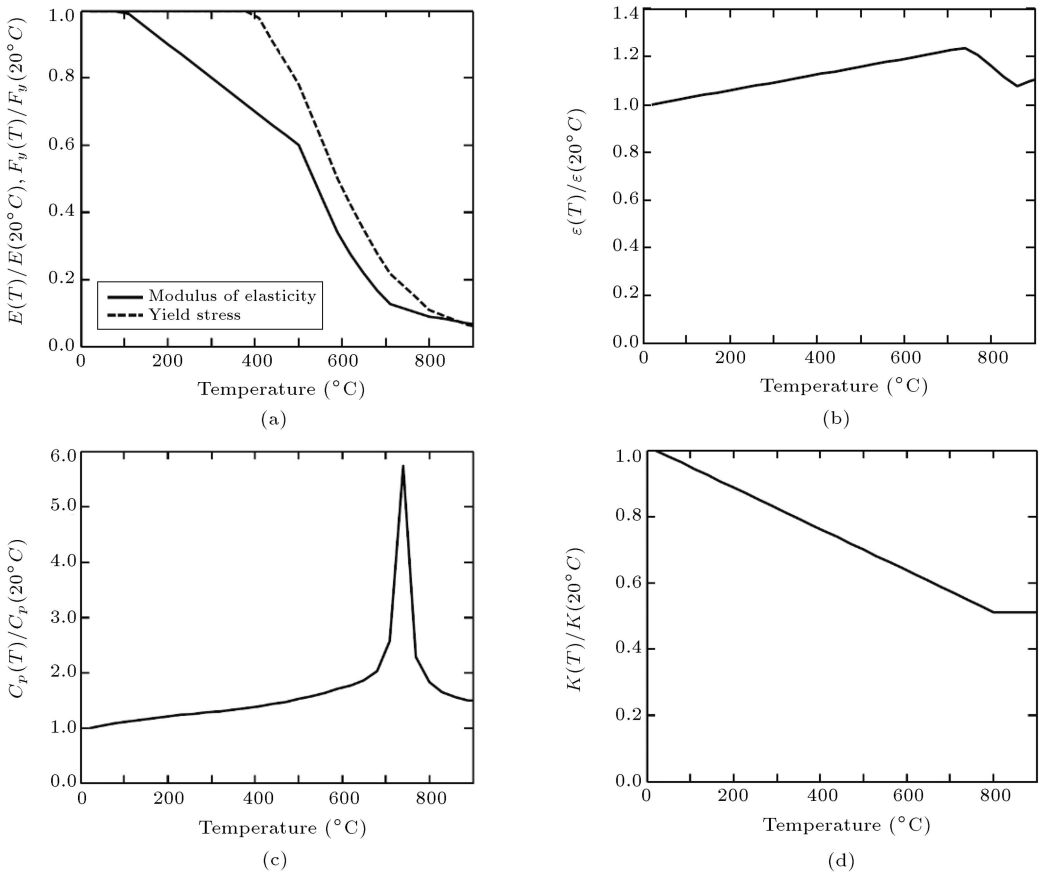

Figure 1. Temperature-dependent mechanical, thermal, and deformational properties of structural steel: (a) Change in the modulus of elasticity and strength, (b) change in the thermal expansion, (c) change in the specific heat, and (d) change in the thermal conductivity [27].

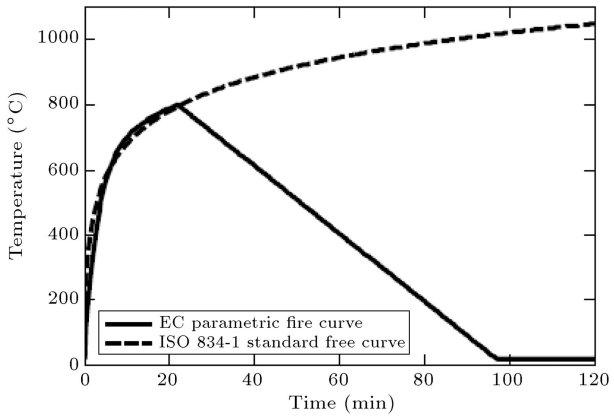

Figure 2. Eurocode parametric fire diagram.

fire growth, the fire diagram will be of ventilation-controlled fire. Then, the cooling phase can be calculated using Eq. (4), which ends before the ambient temperature phase. Ultimately, the ambient temperature after the fire is extinguished and assumed to terminate within 120 min [31].

$$\theta = \theta_{\max} - 625(t^* - t^*_{\max}). \quad (4)$$

In reinforced concrete buildings, the assumption that the temperature generated by the source of fire and that on the surface of structural components are equal cannot be correct. However, this assumption holds for steel structures due to the high conductivity of steel and rapid heat transmission. It is also assumed that for exposed structural components, the temperature distribution across the section is uniform [27].

2.3. Fire scenarios

Determining whether the fire is of travelling or uniform type can significantly affect the structural responses, thus affecting the design and selection of critical components [32]. Herein, to account for the location of fire occurrence, different scenarios for different floors were examined. It is assumed that the structural components are not protected mainly, given the more conservative characteristics of older buildings. The fire was applied only to the unprotected columns, braces, and upper beams of the story exposed to fire since the thermal conductivity of the concrete floor slab prevented heat transfer to the lower beams. According to Quiel Spencer and Garlock [33], the mechanical effects of concrete slabs were ignored in the thermal-mechanical analysis. Given the full composite

action between the concrete slabs and steel girders, rapid thermal expansion created in steel girders caused large tensile forces in concrete slabs and, consequently, formed cracks. Therefore, concrete slabs carry minimum stresses and their structural effects caused by the fire can be neglected [33].

2.4. Verification of the numerical models

For the purpose of validation, a small-scale steel frame, which was tested at high temperatures by Rubert and Schauman [34] and then analyzed by Sun et al. [8], was selected (Figure 3). All structural components are of European-type IPE80-I sections. The left span structural components are uniformly heated according to ISO 834-1 standard fire diagram. Specifications of the applied loads are presented in Figure 3. The model used for validation enjoys Eurocode temperature-dependent material properties [27]. The lateral displacements against temperature are compared at two rigid joints with the experimental and numerical results obtained by other researchers. As seen in Figure 4, there is good agreement between our obtained results and those of previous studies (both numerical and experimental). Therefore, it can be concluded that the proposed modeling and analysis approach can be appropriate for the simulation of the performance of structural steel frames when exposed to fire.

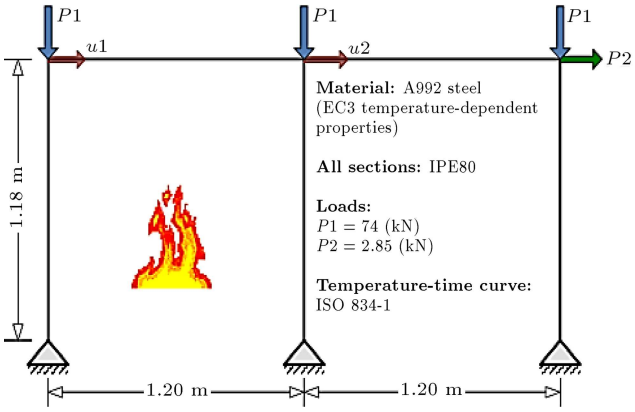

Figure 3. The small-scale steel frame used in the validation of thermal-mechanical analysis [34].

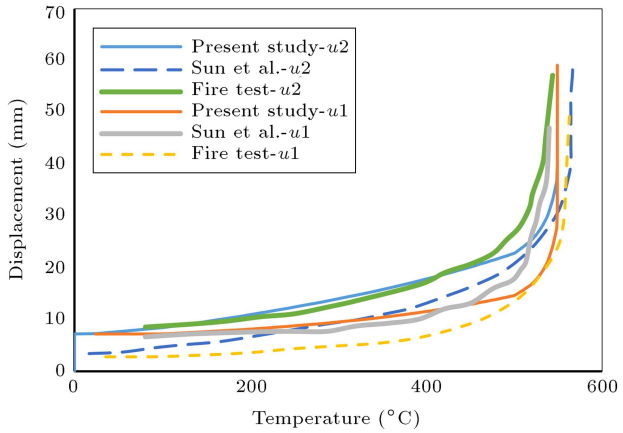

Figure 4. Validation results of the thermal-mechanical analysis.

2.5. Sample building for study

In order to evaluate the performance of NCBF frames when exposed to fire loading, a sample building was selected. The case study here is a building with steel braced frames designed in National Institute of Standards and Technology (NIST) [35] whose response to what may cause progressive collapse is examined in this study. The plan view of the building is shown in Figure 5. The building is a ten-story office with the dimensions of 45.7 m × 45.7 m in the plan and perimeter braced frames as the lateral load-resisting system. Figure 6 shows the East-West perimeter frames of the building selected to be studied. The building is designed to resist moderate earthquakes and it uses SCBF according to AISC seismic provisions [36]. ASCE 7-05 [37] is applicable to design loads. The same structure is designed and assessed as NCBF frame, according to Uniform Building Code (UBC) [23], by the authors. NCBF members and connections were designed using the prescribed seismic forces. There was no consideration of overstrength, its impact on the connection demands, or ductile detailing in this design. This frame is presented in Figure 7. The materials and design standards given in references [36,38–40] are used in the design of the structural components and their connections. The assumed loads for typical floors and roof are shown in Table 1.

The structural building system adopted is comprised of braced frames and gravity system. The

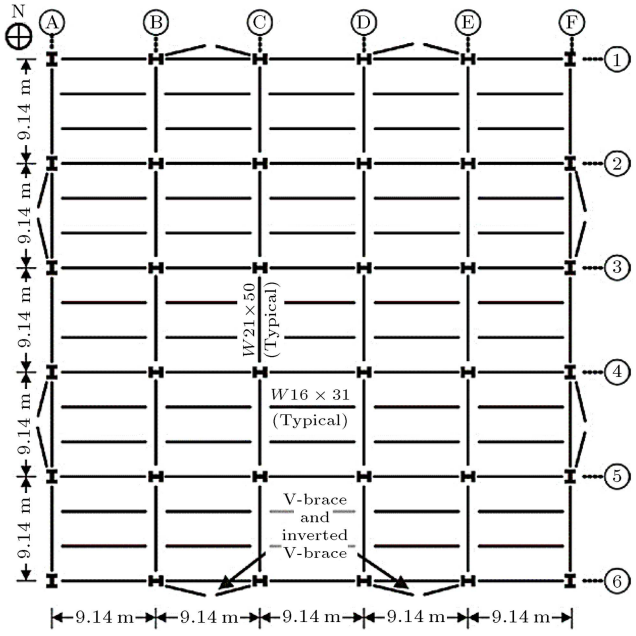

Figure 5. Plan layout for braced frame systems [35].

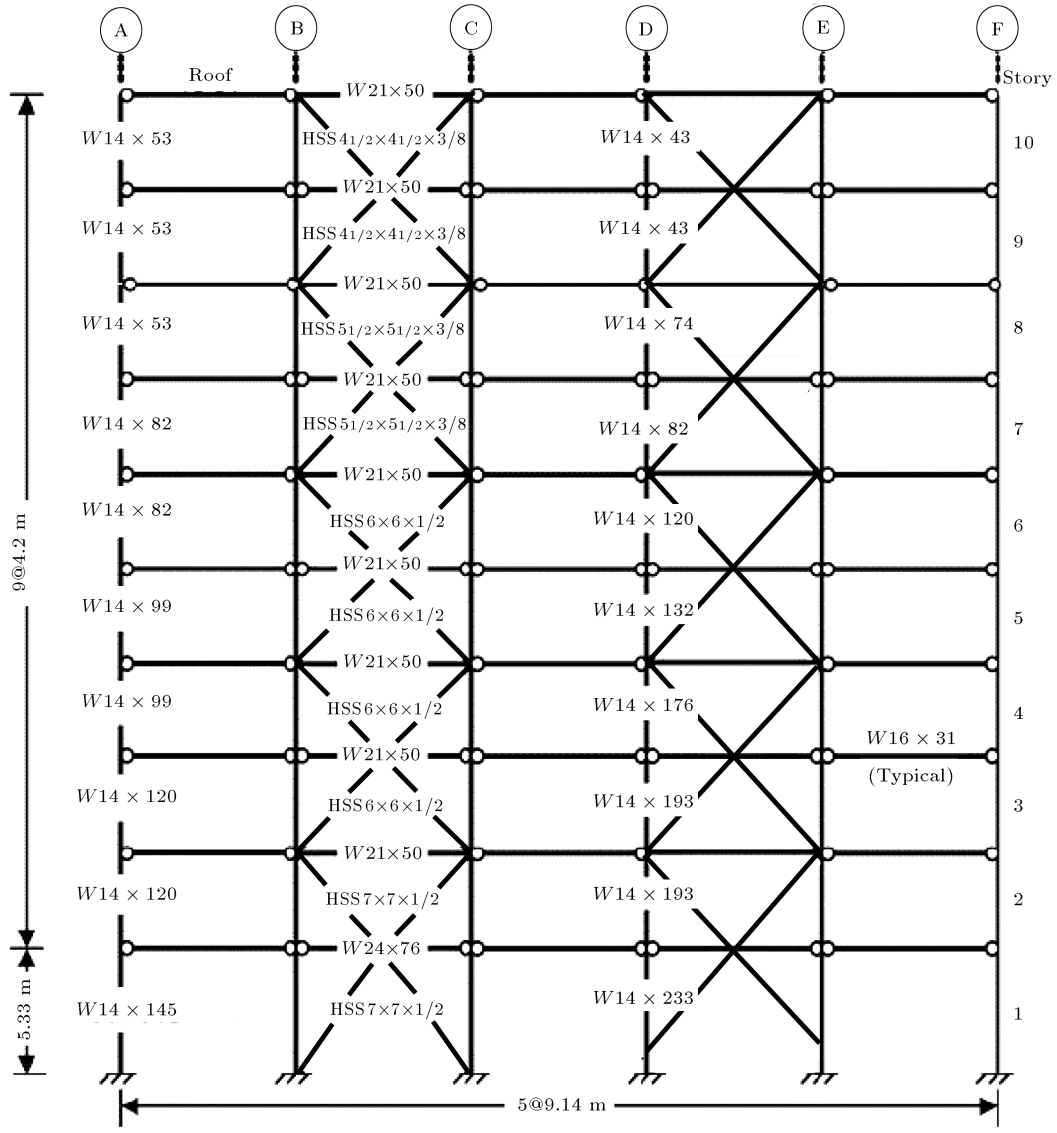

Figure 6. Elevation of Special Concentrically Braced Frame (SCBF) E–W frame (line 6) [35].

Table 1. Assumed loads for typical floors and roof in the case study building.

	Slab self-weight (N/m^2)	Superimposed dead load (N/m^2)	Design live load (N/m^2)
Typical floors	2200	1430	4790
Roof	2200	480	960

columns and beams are connected by shear type connections in the gravity system. The braces are square, seismically compact with Hollow Steel Sections (HSS). While the braces are selected from ASTM A500 grade B steel ($Fy = 317$ MPa), all the beams and columns are of A992 structural steel type ($Fy = 345$ MPa).

2.6. Elements and constraints

The buildings are simplified using two-dimensional slender and initially straight frame elements through two-node Bernoulli beam model [25]. The maximum length used for the finite elements was one m, and the finest mesh of 0.35 m was used around the joints for accurate simulation of plastic hinges formed in the vicinity of beam-column joints. A small initial camber was applied to the middle of the brace to cause buckling. Uriz [41] recommended applying the initial camber at 0.05% and 0.1% distances of the brace length.

For simulating the out-of-plane rotational behavior of connections in the gusset plates, single springs along the brace axial direction were used at both ends of the brace [42]. The initial stiffness of the rota-

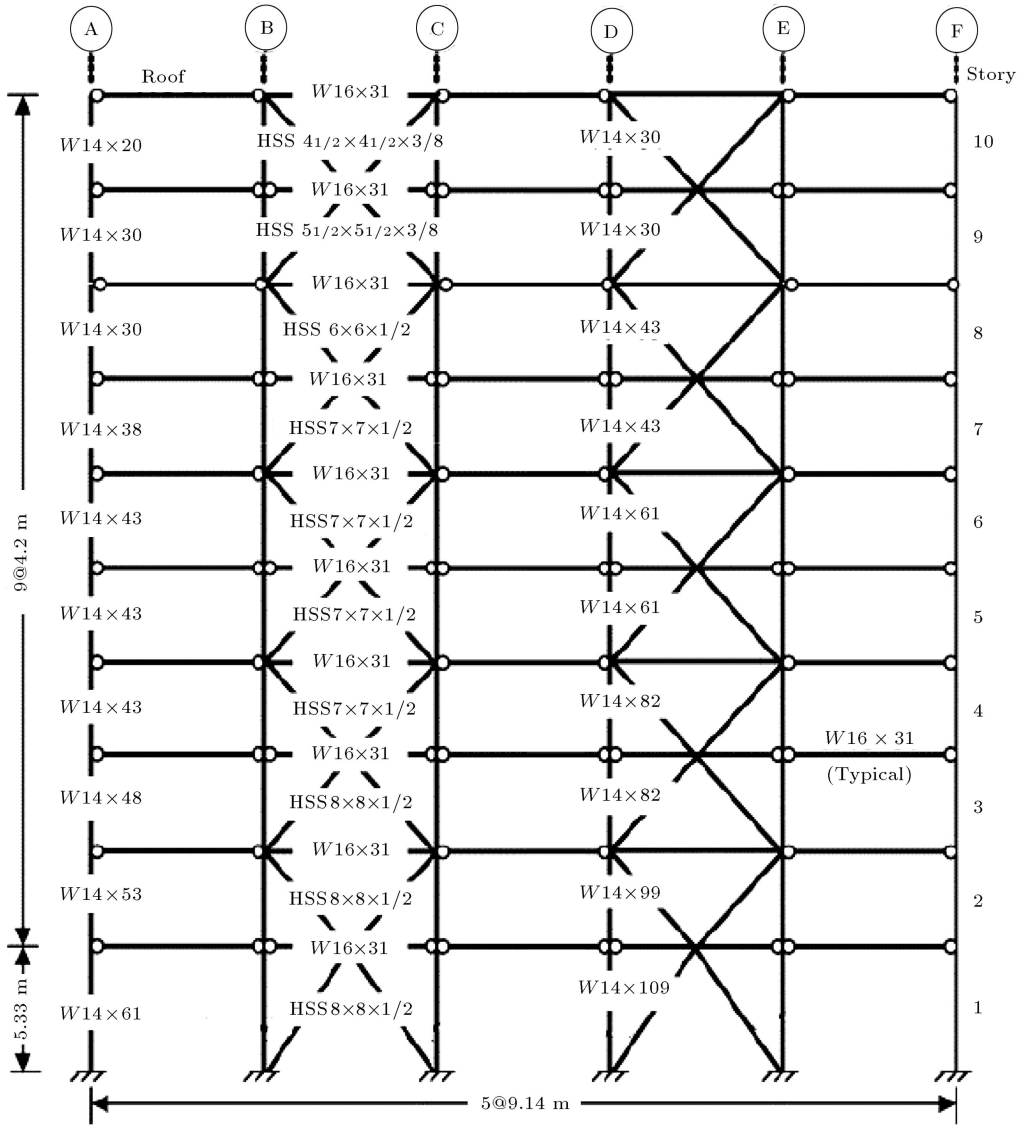

Figure 7. Elevation of Non-seismic Concentrically Braced Frame (NCBF) E–W frame (line 6).

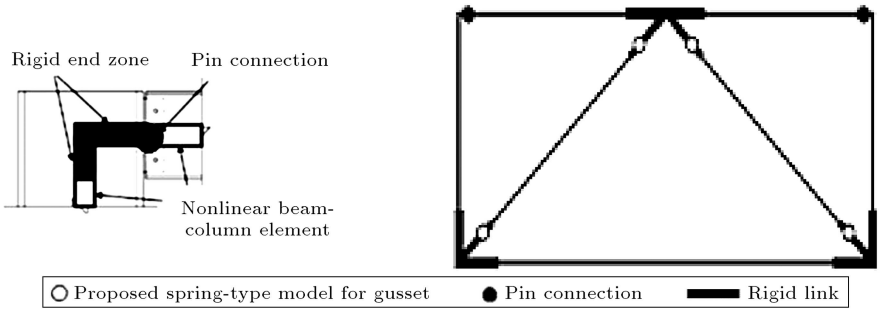

Figure 8. Schematic model of Special Concentrically Braced Frame (SCBF) panel [42].

tional spring was determined based on the gusset plate properties and its geometry. As shown in Figure 8, rigid links were employed to simulate the remainder of the gusset plate. Shear-plate type connection was used for beam-column connections where there was no gusset plate. The beam-column-brace connections were of welded-flange welded-web connection type as they acted as fully restrained with fixed connections. For simplification purposes, all other beam-column connections of the simply pinned type were selected. The columns were fixed at their base so that they could resist lateral forces with a strong axis in the bending di-

rection. Moreover, the beams were laterally supported at the quarter points along the span length. In the beam-to-column and brace-to-frame connections, rigid offsets were used to account the stiffening effect of the gusset plate and physical size of members. The effective length of the braces was equal to 70% of the work-point-to-work-point length. No failure was assumed for the connections in the modelling.

2.7. Loading

The gravity loads are divided into two types of distributed loads corresponding to the gravity loads of brace frame and concentrated loads associated with interior gravity frames (Figure 9). It is necessary to present the gravity frames in leaning columns to demonstrate the $P-\Delta$ effects. For this purpose, a co-rotational method is utilized. As seen in Figure 9, the leaning column is modeled using truss elements. For the connection to the main frame at each floor level, the multi-point constraint rigid links are implemented. The leaning column is pinned at the base and floor levels and it is axially stiff, hence no impact on the lateral stiffness of the main frame. As shown in Figure 10, three different scenarios for three different floors are taken into account: (a) ground floor, (b) fourth floor, and (c) eighth floor. In all of these scenarios, fire loading was applied to the columns, braces, and upper beams of the floor under fire. Further, the floor subjected to fire loading is taken as the fire compartment.

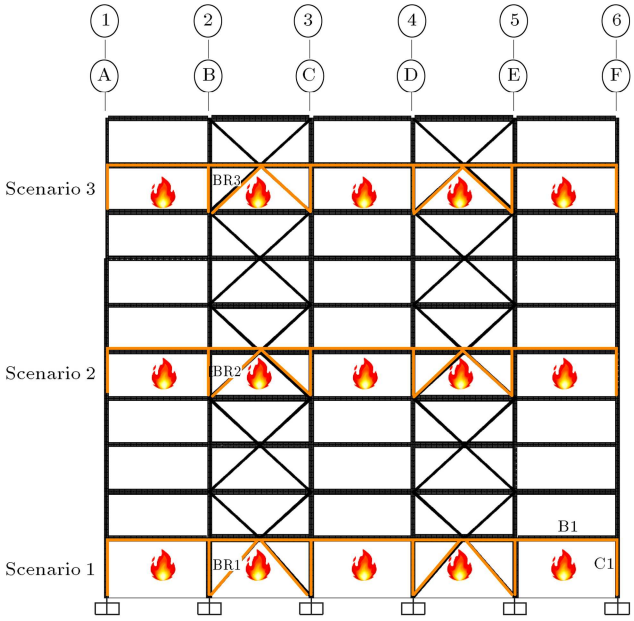

Figure 10. Fire scenarios.

3. Analysis results

In the present study, one of the most important observations regarding the behavior of steel concentrically braced frames exposed to fire was the loss of resistance and structural integrity against fire over a short period of time. In addition, according to these observations, the time duration of resistance against fire was

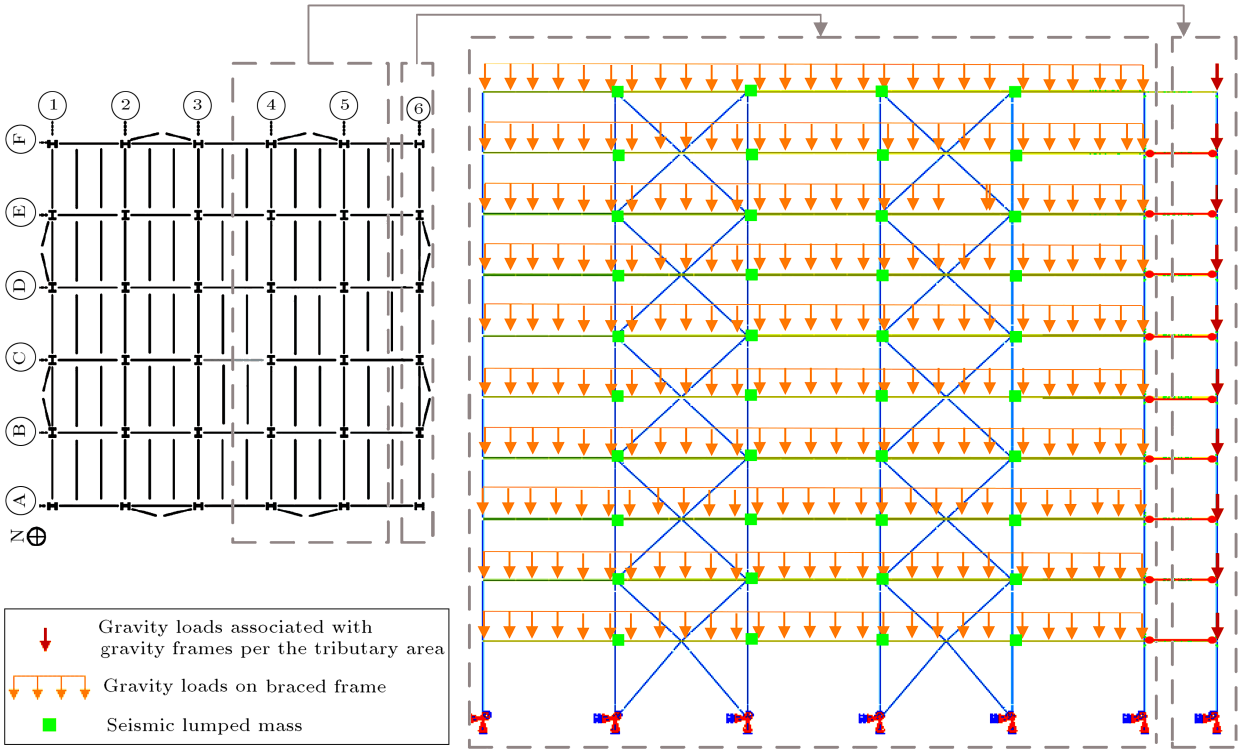

Figure 9. Finite element model of the steel braced frame for illustration.

significantly lower for NCBF than that for SCBF. Figure 11 shows the resistance of the structure to fire in Scenario 1 when the fire is uniformly applied to the ground floor. The fire resistance is defined as the time duration in which the displacements, either globally or locally, exceed the chosen thresholds. The thresholds were identified by displacements versus time step curve merging towards the vertical asymptote [43]. Based on the above-mentioned information, Figures 11–13 show time versus lateral displacement in the upper slab of the floor under Fire Scenarios 1–3. According to Figure 11, the fire resistance of the SCBF sample based on Scenario 1 lasted approximately 10 minutes and 31 seconds, while the fire resistance of the NCBF based on Scenario 1 lasted approximately 7 minutes and 15 seconds. The lateral displacement versus time

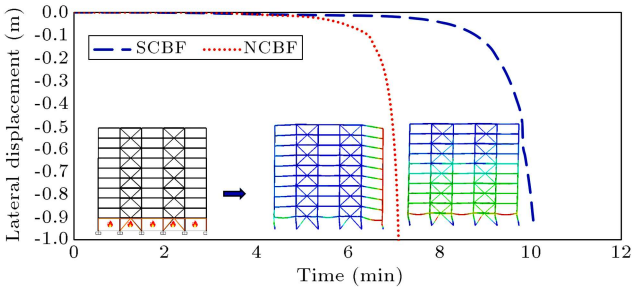

Figure 11. Fire resistance for Special Concentrically Braced Frame (SCBF) and Non-seismic Concentrically Braced Frame (NCBF) based on Scenario 1.

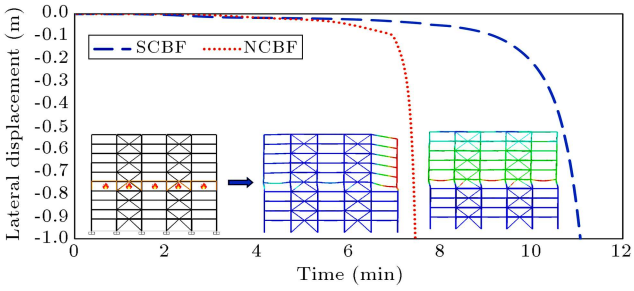

Figure 12. Fire resistance for Special Concentrically Braced Frame (SCBF) and Non-seismic Concentrically Braced Frame (NCBF) based on Scenario 2.

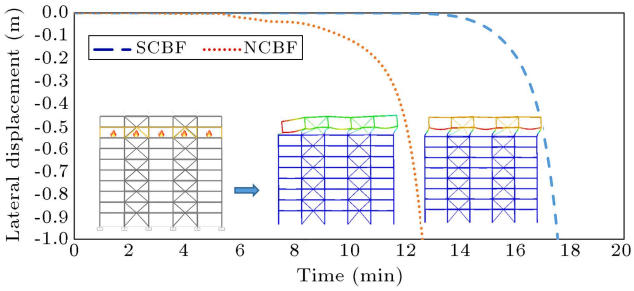

Figure 13. Fire resistance for Special Concentrically Braced Frame (SCBF) and Non-seismic Concentrically Braced Frame (NCBF) based on Scenario 3.

based on Scenario 2 is given in Figure 12. In this figure, the fire resistance of the SCBF sample was insignificantly different from that of the prior case, which was approximately 11 minutes and 33 seconds. The fire resistance of the NCBF sample based on Scenario 2 was approximately 7 minutes and 30 seconds. Fire resistance based on Scenario 3 is shown in Figure 13. The fire resistance of the SCBF frame based on the uniform fire applied to the eight floors was lost in about 18 minutes and 39 seconds, and it consequently led to collapse, while the fire resistance of the NCBF frame was about 13 minutes and 36 seconds.

One of the main findings of the behavior of the steel braced frame elements subjected to fire is the internal forces generated due to the heated beams, which exceed the yield threshold at high temperatures. This occurs due to the large compressive axial forces developed as a result of lateral constraints on the expansion of beams. Large axial forces are generated in the beams when subjected to the heating phase, and the axial expansion causes considerable moments in columns at both beam ends. Therefore, examining the interaction between axial forces and bending moment in beams and columns is essential to assessing their performance during the fire. Eq. (5) [38], which represents the axial force-bending moment interaction, is applied to the chosen braced frame beams and columns:

$$\frac{P_r(T)}{2P_n(T)}+\frac{M_r(T)}{M_n(T)}\leq 1 \qquad \text{for} \quad \frac{P_r(T)}{P_n(T)}<0.2,$$

$$\frac{P_r(T)}{P_n(T)}+\frac{8M_r(T)}{9M_n(T)}\leq 1 \qquad \text{for} \quad \frac{P_r(T)}{P_n(T)}\geq 0.2. \tag{5}$$

In the above equation, $P_n(T)$ and $M_n(T)$ denote the compressive or tensile and flexural strengths of members as a function of temperature, respectively. Calculations of $P_n(T)$ and $M_n(T)$ are based on AISC 360-05 specification. In addition, $P_r(T)$ and $M_r(T)$ are the axial compressive or tensile force and bending moment of the structural components, respectively, which are the functions of the temperature. The internal forces developed in some of the heated beams for the fire scenarios are shown in Figures 14 and 15. The axial force history of the specified elements was placed into the bending-axial interaction equation to demonstrate the bending capacity of the element as a function of time.

The history of axial force in the beams subjected to heat indicates that at the heated phase, an increase in the compressive axial force makes the internal forces reach the yield interaction threshold. In other words, at this temperature, the interactions of the internal forces go beyond the curve of the interaction, as seen in Eq. (5). The interaction ratio in Eq. (5) for the

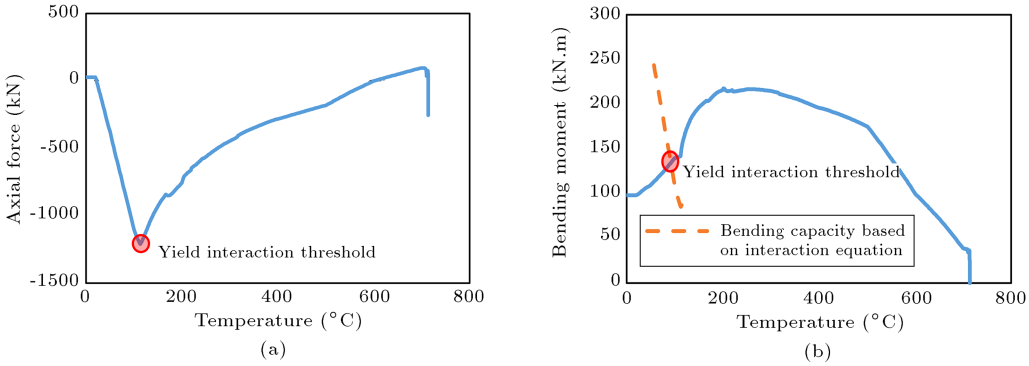

Figure 14. History of internal forces in the mid-span of B1 beam based on Scenario 1 for Non-seismic Concentrically Braced Frame (NCBF): (a) Axial forces time history and (b) bending moment time history.

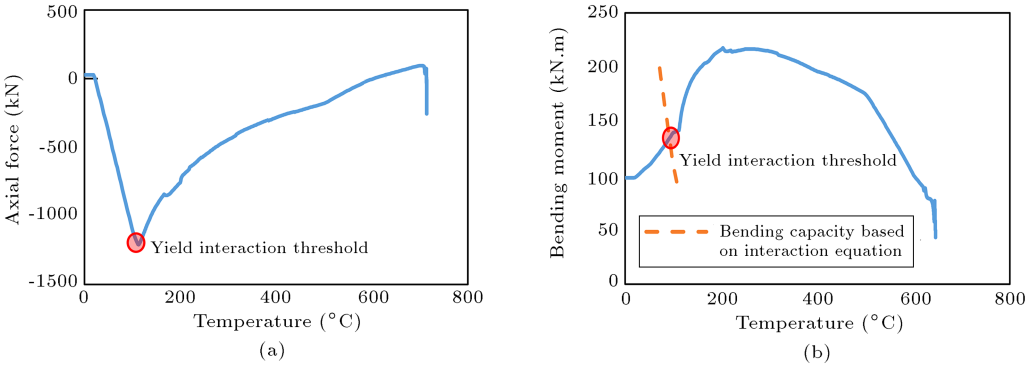

Figure 15. History of internal forces in the mid-span of B1 beam based on Scenario 1 for Special Concentrically Braced Frame (SCBF): (a) Axial forces time history and (b) bending moment time history.

B1 beam (as specified in Figure 10) at a temperature of 110°C reaches the yield interaction threshold. Moreover, as the modulus of elasticity considerably decreased, the compressive axial force was also reduced, reaching almost zero axial compressive force at almost 600°C. The reduction of the compressive axial forces in beams was particularly intensified at 500°C when the modulus of elasticity suddenly declined.

Figures 16 and 17 present the internal forces developed in C1 column (demonstrated in Figure 10) under Fire Scenario 1. In addition, by placing the axial force history of this element in the bending-axial interaction equation, the bending capacity of the element at the yield interaction threshold is shown as a function of temperature. As observed, upon increasing temperature and consequently decreasing column axial stiffness, the bending capacity of the column would decrease. The interaction ratios (Eq. (5)) of C1 column before the occurrence of fire for NCBF and SCBF frames were 0.44 and 0.06, respectively. Followed by the fire, the mentioned values reached the threshold yields at temperatures of about 640°C and

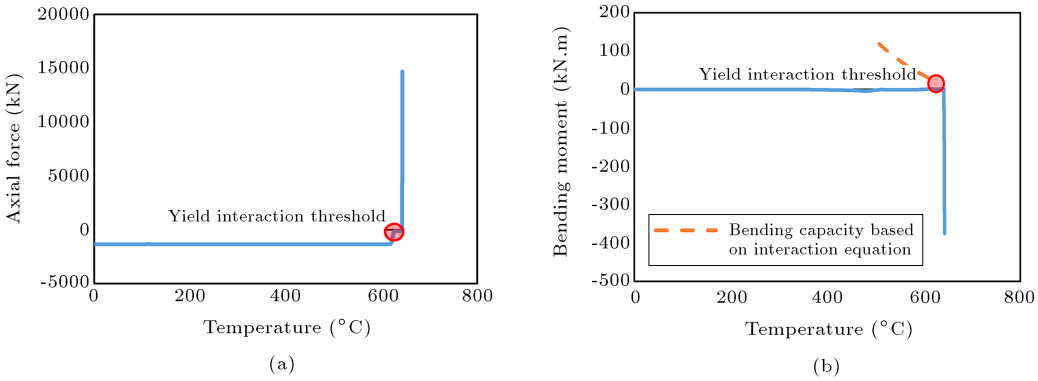

Figure 16. History of internal forces in sec. 1-1 of C1 critical column during Scenario 1 for Non-seismic Concentrically Braced Frame (NCBF): (a) Axial forces time history and (b) bending moment time history.

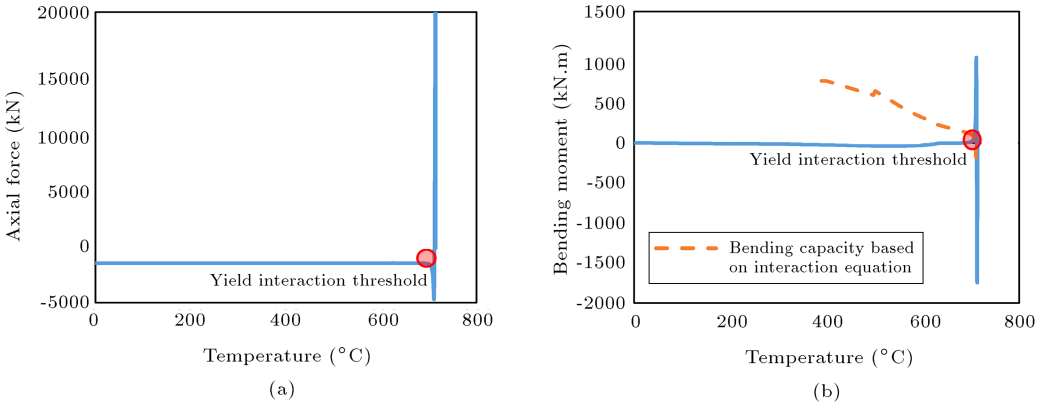

Figure 17. History of internal forces in sec. 1-1 of C1 critical column during Scenario 1 for Special Concentrically Braced Frame (SCBF): (a) Axial forces time history and (b) bending moment time history.

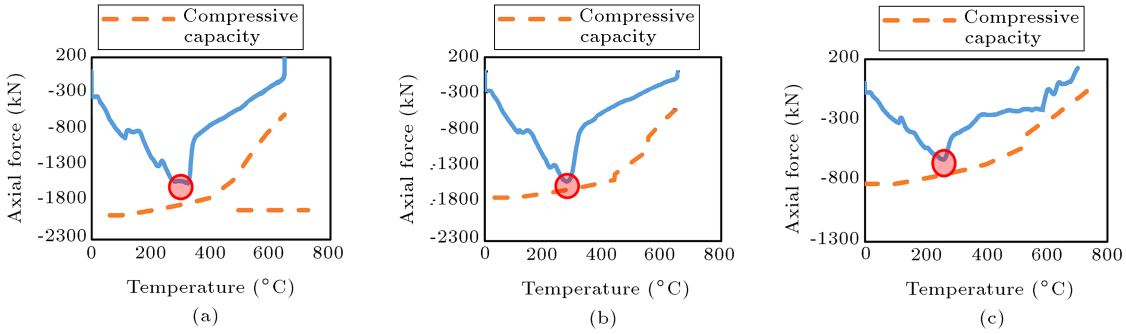

Figure 18. Axial force time history in the critical braces of Non-seismic Concentrically Braced Frame (NCBF): (a) BR1 brace in Scenario 1, (b) BR2 brace in Scenario 2, and(c) BR3 brace in Scenario 3.

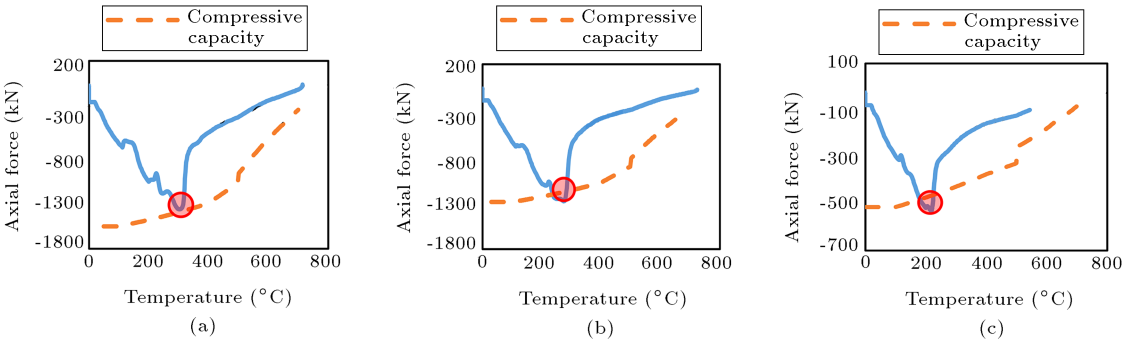

Figure 19. Axial force time history in the critical braces of Special Concentrically Braced Frame (SCBF): (a) BR1 brace in Scenario 1, (b) BR2 brace in Scenario 2, and (c) BR3 brace in Scenario 3.

720°C. Then, the column collapsed due to the lateral displacement and $P-\Delta$ effect.

To evaluate the behavior of braces, the history of the internal axial forces developed in some of the heated braces (specified in Figure 10) of different scenarios in both samples was extracted, as shown for NCBF in Figure 18 and SCBF in Figure 19. Moreover, the buckling load of braces was calculated based on AISC 360-05 [36,38], as shown in the diagrams of Figures 18 and 19. As observed in both frames, the increased temperature is associated with the higher axial expansion of the braces and their compressive axial force. As the braces reached their buckling load, they lost their resistance. The axial forces for BR1, BR2, and BR3 braces before the occurrence of fire were negligible. After the occurrence of fire, they reached the buckling load at temperatures of about 320°C, 270°C, and 220°C for NCBF frame and 320°C, 270°C, and 220°C for SCBF frame. As a result, increased temperature and asymmetric deformation of the structure, as well as the effect of $P-\Delta$, caused an increase in the relative lateral displacement of the floor, thus leading to tensile forces in some pre-buckled braces. As the tensile forces increased in the braces and

reached the ultimate tensile capacity, the braces broke down and the floor collapsed as a result of the loss of the resistance of the columns under fire.

4. Summary and conclusion

In this study, the performance of the two samples of concentrically braced frames (Non-seismic Concentrically Braced Frame (NCBF) and Special Concentrically Braced Frame (SCBF)) subjected to fire was evaluated under three different fire scenarios. The following conclusions could be drawn from the analyses:

- By changing the fire scenario from the lower floors to the upper floors would increase the durability of the structure's resistance to fire. For instance, in the NCBF frame, the fire resistance time increased from 7 minutes and 15 seconds per fire on the ground floor to 13 minutes and 36 seconds per eighth floor fire. In the SCBF frame, the resistance time also increased from 10 minutes and 31 seconds in the case of fire on the ground floor to 18 minutes and 39 seconds in the case of fire on the eighth floor. This could be due to the reduced load ratio of the column as well as the effect of $P-\Delta$ on higher levels, which in turn affected the collapse of the structure. As a result, the fire scenario for the lower floors could increase the risk of early collapse;
- According to the observations, the time duration of resistance under different fire scenarios was lower for the NCBF frame than that for the SCBF frame. The time duration of resistance for Scenarios 1, 2, and 3 in the SCBF sample decreased from 10 minutes and 31 seconds, 11 minutes and 31 seconds, and 18 minutes and 39 seconds to 7 minutes and 15 seconds, 7 minutes and 30 seconds, and 13 minutes and 36 seconds in the NCBF sample, respectively;
- The results revealed that the ratio of the bending-axial interaction for the gravity beams was about 0.30 before the fire event. However, the axial compressive force of beams at the beginning of the heated phase increased due to the expansion. Consequently, after the fire occurrence, the bending-axial interaction of beams reached the yield threshold at a temperature of about 110°C. Then, due to a significant decrease in the modulus of elasticity, a reduction was observed in the compressive axial force;
- Different fire scenarios demonstrated that the reduction of the column axial stiffness would result in the buckling of the columns at high temperatures. For instance, the bending-axial interaction ratios for the ground corner columns before the occurrence of fire for NCBF and SCBF frames were 0.44 and 0.06, respectively, and after the occurrence of fire, they reached the yield threshold at temperatures of about 640°C and 720°C, respectively;
- A thorough examination of the history of the axial forces in the braces exposed to fire indicated that the compressive axial force increased upon increase in the temperature. This phenomenon is followed by the loss of their resistance when reaching the buckling load. For instance, the pre-fire axial force was negligible for the BR1, BR2, and BR3 braces in both of the samples. After the fire incidence, the axial forces of the BR1, BR2, and BR3 braces in the NCBF frame at temperatures of about 325°C, 280°C, and 260°C and in the SCBF frame at temperatures of about 315°C, 265°C, and 220°C reached their buckling load, respectively.

References

1. O'Connor, M.A. and Martin, D.M. "Behaviour of a multi-storey steel framed building subjected to fire attack", *Journal of Constructional Steel Research*, **46**, pp. 295–295 (1998).
2. Gu, L. and Kodur, V. "Role of insulation effectiveness on fire resistance of steel structures under extreme loading events", *Journal of Performance of Constructed Facilities*, **25**(4), pp. 277–286 (2011).
3. Huang, Z., Burgess, I.W., and Plank, R.J. "Three-dimensional analysis of composite steel-framed buildings in fire", *Journal of Structural Engineering*, **126**(3), pp. 389–397 (2000).
4. Liew, J.Y.R. and Ma, K.Y. "Advanced analysis of 3D steel framework exposed to compartment fire", *Fire and Materials*, **28**(2–4), pp. 253–267 (2004).
5. Saab, H.A. and Nethercot, D.A. "Modelling steel frame behaviour under fire conditions", *Engineering Structures*, **13**(4), pp. 371–382 (1991).
6. Wang, Y.C. and Moore, D.B. "Steel frames in fire: Analysis", *Engineering Structures*, **17**(6), pp. 462–472 (1995).
7. Alderighi, E. and Salvatore, W. "Structural fire performance of earthquake-resistant composite steel-concrete frames", *Engineering Structures*, **31**(4), pp. 894–909 (2009).
8. Sun, R., Huang, Z., and Burgess, I.W. "Progressive collapse analysis of steel structures under fire conditions", *Engineering Structures*, **34**, pp. 400–413 (2012).
9. Jiang, J. and Li, G.Q. "Progressive collapse analysis of 3D steel frames with concrete slabs exposed to localized fire", *Engineering Structure Journal*, **149**, pp. 21–34 (2017).
10. Jiang, B.H., Li, G.Q., Li, L.L., et al. "Simulations on progressive collapse resistance of steel moment frames under localized fire", *Journal of Constraction Steel Research*, **138**, pp. 380–388 (2017).

11. Jiang, J. and Li, G.Q. "Disproportional collapse of 3D steel-framed structures exposed to various compartment fires", *Journal of Constraction Steel Research*, **138**, pp. 594–607 (2017).

12. Wong, M.B. "Plastic frame analysis under fire conditions", *ASCE's Journal of Structural Engineering*, **127**(3), pp. 290–295 (2001).

13. Wong, M.B. "Elastic and plastic methods for numerical modelling of steel structures subject to fire", *Journal of Constructional Steel Research*, **57**(1), pp. 1–14 (2001).

14. Fang, C., Izzuddin, B.A., Obiala, R., et al., "Robustness of multi-storey car parks under vehicle fire", *Journal of Constraction. Steel Research*, **75**, pp. 72–84 (2012).

15. Fang, C., Izzuddin, B.A., Elghazouli, A.Y., et al. "Robustness of multi-storey car parks under localised fire towards practical design recommendations", *Journal of Constriction. Steel Research*, **90**, pp. 193–208 (2013).

16. Fang, C., Izzuddin, B.A., Elghazouli, A.Y., et al. "Simplified energy-based robustness assessment for steel-composite car parks under vehicle fire", *Engineering Structure Journal*, **49**, pp. 719–732 (2013).

17. Lange, D., Roben, C., and Usmani, A.S. "Tall building collapse mechanisms initiated by fire: mechanisms and design methodology", *Engineering Structure Journal*, **36**, pp. 90–103 (2012).

18. Sun, R.R., Huang, Z.H., and Burgess, I. "The collapse behaviour of braced steel frames exposed to fire", *Journal of Constriction. Steel Research*, **72**, pp. 130–142 (2012).

19. Behnam, B. "Failure sensitivity analysis of tall moment-resisting structures under natural fires", *International Journal of Civil Engineering*, **16**(12), pp. 1771–1780 (2017).

20. Behnam, B. "Fire structural response of the Plasco building: A preliminary investigation report", *International Journal of Civil Engineering*, **17**, pp. 563–580 (2018).

21. Memari, M. and Mahmoud, H. "Multi-resolution analysis of the SAC steel frames with RBS connections under fire", *Fire Safety Journal*, **98**, pp. 90–108 (2018).

22. Lou, G., Wang, C., Jiang, J., et al. "Fire tests on full-scale steel portal frames against progressive collapse", *Journal of Constructional Steel Research*, **145**, pp. 137–152 (2018).

23. Uniform Building Code, ICBO, Whittier, California (1988).

24. Behnam, B. and Ronagh, H.R. "Post-earthquake fire performance-based behaviour of unprotected moment resisting 2D steel frames", *KSCE Journal of Civil Engineering*, **19**(1), pp. 274–284 (2014).

25. Dassault Systèmes Simulia Corp, ABAQUS 6.14 Documentation, Dassault Systèmes Simulia Corp: RI, USA (2014).

26. ASCE 7-10: *Minimum Design Loads for Buildings and Other Structures*, American Society of Civil Engineers, Virginia, US (2010).

27. EN 1993-1-2, Eurocode3: *Design of Steel Structures, Part1-2: GeneralRules-Structural Fire Design*, European Committee for Normalization (2005).

28. Arasaratnam, P., Sivakumaran, K.S., and Tait, M.J. "True stress-true strain models for structural steel elements", *International Scholarly Research Network*, **2011**, pp. 1–11 (2011). https://doi.org/10.5402/2011/656401

29. ISO 834: *Fire Resistance Test Elements of Building Construction*, International Organization for Standardization (1999).

30. EN 1991-1-2, Eurocode1: *Action on Structures* - Part 1-2: *General Actions - Actions on Structures Exposed to Fire*, European Committee for Normalization (2002).

31. Memari, M., Mahmoud, H., and Ellingwood, B. "Post-earthquake fire performance of moment resisting frames with reduced beam section connections", *Journal of Constructional Steel Research*, **103**, pp. 215–229 (2014).

32. Rackauskaite, E., Kotsovinos, P., Jeffers, A., et al., "Structural analysis of multi-storey steel frames exposed to travelling fires and traditional design fires", *Engineering Structures*, **150**, pp. 271–287 (2017).

33. Quiel Spencer, E. and Garlock, E.M. "Modeling high-rise steel framed buildings under fire", In *ASCE Structures Congress* (2008).

34. Rubert, A. and Schaumann, P. "Tragverhalten stählerner Rahmensysteme bei Brandbeanspruchung", *Stahlbau.*, **54**, pp. 280–287 (September 1985).

35. Ghosh, S.K., *Assessing Ability of Seismic Structural Systems to Withstand Progressive Collapse: Design of Steel Braced Frame Buildings*, The National Institute of Standards and Technology (2006).

36. ANSI/AISC 341-05: *Seismic Provisions for Structural Steel Buildings*, American Institute of Steel Construction, Chicago, US (2005).

37. ASCE 7-05: *Minimum Design Loads for Buildings and other Structures*, American Society of Civil Engineers, Virginia, US (2005).

38. ANSI/AISC 360-05: *Specifications for Structural Steel Buildings*, American Institute of Steel Construction, Chicago, US (2005).

39. *AISC Steel Construction Manual*, American Institute of Steel Construction, Chicago, US (2006).

40. International Building Code (IBC), International Code Council (2006).

41. Uriz, P., *Towards Earthquake Resistant Design of Concentrically Braced Steel Structures*, University of California: Berkeley, California (2005).

42. Hsiao, P.C., Lehman, D.E., and Roeder, C.W. "Improved analytical model for special concentrically braced frames", *Journal of Constructional Steel Research*, **73**, pp. 80–94 (2012).

43. Almand, K., Phan, L., McAllister, T., et al. "NETSFPE workshop for development of a national R&D roadmap for structural fire safety design and retrofit of structures", NlSTlR 7133 National Institute of Standards and Technology (2004).

Biographies

Mohammad Rasul Kaffash received his PhD in Structural Engineering from Ferdowsi University of Mashhad in 2019. He is working at a civil engineering company as a consultant engineer. His major specialty is structural fire engineering and modeling of structural systems.

Abbas Karamodin is an Associate Professor of Civil Engineering at Ferdowsi University of Mashhad. He received his PhD from Ferdowsi University of Mashhad. His studies cover a wide range of topics in the structural and earthquakes engineering including structural control, performance-based engineering, and fire engineering.

Mohammad Moghiman is a Professor of Mechanical Engineering at Ferdowsi University of Mashhad. He received his PhD from Wales University in 1990. His studies cover a wide range of topics in the mechanical engineering including combustion, evaporation, simulation, and air conditioning.